ANALYSIS OF DIFFERENT MICROFLUIDIC PIN-FIN STRUCTURES IN METAL ADDITIVELY MICROFABRICATED PACKAGESFOR THERMAL MANAGEMENT OF MICROSYSTEMS

Bhushan Lohani[1], Ryan M. Price[2], Peter Sanchez[2] and Robert C. Roberts[2]
[1]Pennsylvania State University, State College, Pennsylvania, USA
[2]The University of Texas at El Paso, El Paso, Texas, USA

ABSTRACT

This study explores and compares the thermal performance of three microfluidic micro-pin-fin structures on metal additively microfabricated packages for semiconductor die thermal management. Direct Metal Laser Sintering (DMLS) is utilized in this work to fabricate the packages. This work not only showcases the potential of additive manufacturing in fabricating microfluidic packages but also upon their integration with cleanroom microfabricated semiconductor dies allows for heterogeneous integration of diversely fabricated components. Efficient heat dissipation from the dies is achieved through fluid flow within the microfluidic structures, enhancing functionality and operation. This concept embodies heterogeneous integration, highlighting the combination of diverse fabrication processes and functional enhancements.

KEYWORDS

Direct Metal Laser Sintering, Microfluidics, Packaging, Thermal Management, Heat Exchanger

INTRODUCTION

The ongoing trend toward miniaturization of microsystems, aimed at cramming more functionality into smaller die sizes for compact and high-performance devices, has given rise to higher current and power densities as well as localized heat generation, or hotspots, within the chips [1]. As illustrated in [2] problems exist with the use of wide and ultra-wide bandgap semiconductors as elevated temperatures heat degrade the materials leading to premature failure and potentially to thermal runaway. The trend towards 3D heterogeneous integration has transformed electronics packaging into a complex microsystem itself, requiring innovation. Local hotspots, created by dense active circuitry, elevate the die temperature, adversely affecting reliability, performance, and the ultimate lifespan of the devices. Effective thermal management of devices is crucial to fully harness the benefits of miniaturization obtained after several decades of research and development. Traditional system-level cooling methods, like copper or aluminum heat exchangers, fins, and fans, rely on conductive heat transfer through interfaces. In addition, these limitations often require spreading heat over a larger area to be effective. These passive spreader devices are commonly seen in a growing number of devices with the most familiar being computers and vehicle parts. They are easily available and have established usages but suffer from higher thermal resistance and increases hardware size and costs [3].

Die-level thermal management systems, such as microfluidic channels and micro pin-fins on the back end of the die, offer efficient cooling due to direct contact [4], [5]. The introduction of efficient cooling systems like microfluidic channels with higher convective heat transfer coefficient in the closer proximity of the hotspot imparts better thermal management compared to conductive system level heat sinks. However, their implementation poses yet another design and fabrication burden to the already complicated semiconductor fabrication processes as well as the die. Fabrication methods for these channels varies greatly with advantages and disadvantages to each [6], [7], [8], [9], [10]. To realize the benefits of these methods without burdening the die, this paper proposes an innovation in die packaging. Current electronic packages, typically made from metal plates via stamping or etching, include leads for electrical connection, a die pad for die support, and epoxy for assembly and die isolation from external contaminants. Integrating microfluidic structures onto the extended die pad offers effective package-level thermal management [11], [12], [13]. Our initial work in [11] demonstrated feasibility of the approach, and our other works in [12], [13] explored the impact of optimization of fluidic channel based cooling designs.

This approach streamlines thermal management by leveraging the existing die pad for direct cooling while minimizing additional fabrication complexity. By incorporating microfluidic structures into the package design, heat dissipation is significantly improved, enhancing device reliability and performance without increasing size or cost.

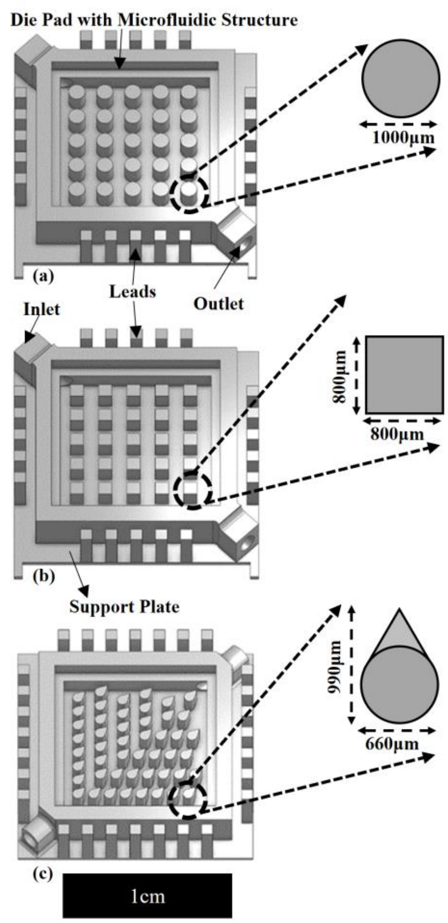

Figure 1: CAD file renderings of packages with circular (a), square (b), and teardrop (c) micro pin-fins with dimensions of each of them in inset.

In this paper a comparative study of three different microfluidic pin-fin structures as shown in Figure 1 is detailed. The cooling efficacy of these microfluidic structures is dictated by the flow resistance and surface area of contact which will be demonstrated later in this paper. With the alteration of micro pin-fin design from circular pin-fin to a more hydrodynamic teardrop pin-fin, it was possible to reduce the overall thermal resistance of the whole system from around 1.1W/°C for the former to 0.9W/°C for the latter. Both of which are much lower compared to 5.25W/°C for a package without these kinds of microfluidic structures [5].

DESIGN AND FABRICATION

Direct Metal Laser Sintering (DMLS) was employed to additively microfabricate the packages tested in this work. The advantage of using additive microfabrication is that with proper design of the parts as well as support structure a wide variety of structures can be fabricated based on 3-Dimensional (3D) Computer-Aided Design (CAD) file. The CAD design of the packages with circular pin fin (CPF), square pin fin (SPF), and tear-drop pin-fin (TDPF) are shown in the left side of Figure 1 (a), (b), and (c) respectively. These were designed on Onshape™ CAD 3D modelling software. The packages are designed to hold a 1cm by 1cm semiconductor die on the die pad. The die pad has microfluidic pin-fin structure below the proposed location of the die. The packages are also designed with electrically isolatable lead pin pads for die connectivity once encapsulated. All the pin-fins are 1.25mm in height. The circular pin-fin is 1mm in diameter, the square pin fin is 0.8mm by 0.8mm in length, and the tear-drop pin fin has the dimensions as shown in Figure 1.

Microfabrication was performed using the Xact Metal™ XM200C, a Direct Metal Laser Sintering printer. The XM200C has a laser spot size of 20µm or greater and a build platform measuring 127mm by 127mm, capable of printing parts slightly below 127mm in height. The printer sinters together layers of 30µm in each pass and it supports printing using metal powders such as 316L, 17-4PH, 15-5, 400 Stainless Steel, bronze, and cobalt chrome precursor powder. In this study, 316L stainless steel powder (Praxair) with a diameter ranging from 30-100µm was utilized. As-received powder was preprocessed through a 45µm mesh vibratory sieve to remove larger diameter powder from the system prior to manufacturing.

The prefabrication process involves slicing the designed package CAD file into multiple layers and generating toolpaths for the printer using the Autodesk Netfabb slicing software. After generating a viable toolpath and verifying correctness using a build simulation, this toolpath is loaded onto the DMLS printer. The build is started, fabrication commences by spreading a 30µm layer of powder metal, pre-loaded into the printer, from the powder bed to the pre-flattened and level build plate using a recoater blade. Regions of layers are selectively sintered and fused according to the sliced CAD model file. This process of layering and selective sintering is repeated until the full 3D structure is fabricated. However, the 3D part is fused to the build plate and requires mechanical separation. Figure 2 depicts the fabricated and released packages utilized in this study. Material property characterization of these parts as printed using the aforementioned DMLS process was conducted and detailed in previous work [12].

As seen in Figure 1, Figure 2, and mentioned previously, the package die pad and lead are fabricated on top of a support structure to hold the parts in place. Once the die is placed on the die pad, wire bonded, and epoxy cured, the support structure can be removed as shown in Figure 3. This process was completed with a surface grinder. Once all fabrication steps are done, the leads are electrically isolated. The back side of the of the package as fabricated is shown in Figure 4.

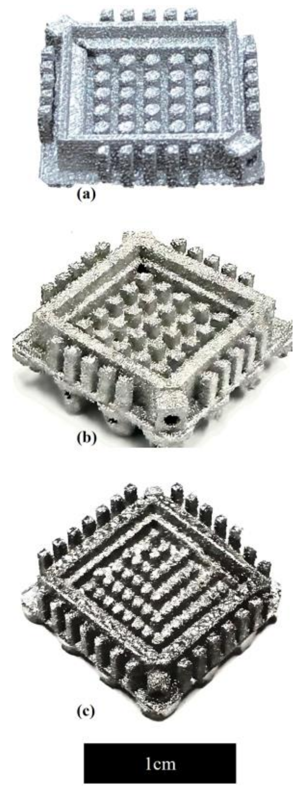

Figure 2: 316L Stainless steel packages microfabricated using DMLS Process. Circular (a), square (b), and teardrop (c) micro pin-fins.

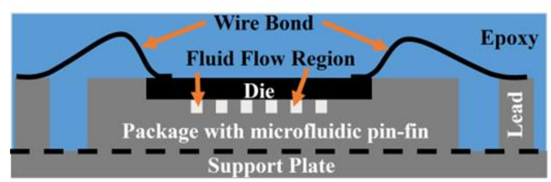

Figure 3: Cartoon illustration of the proposed die integration where the die is placed on the die holder, die pads wire bonded to respective leads, and the whole system encapsulated in epoxy. Once the epoxy cures, the support plate will be ground off till the broken line electrically isolating the leads.

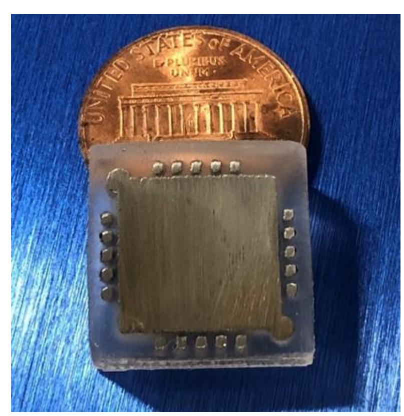

Figure 4: Backside of the final assembled package. The back surface is smooth from the surface finishing and pin isolation

TEST SETUP

Figure 5 depicts the experimental setup. The inlet and outlet fluid ports were extended using 20-gauge blunt needles, as illustrated in Figure 5. A bare silicon interposer was mounted onto the die pad to mimic a real die. The die's edge was securely attached to the package using 2-part epoxy to ensure stability and prevent leakage. With these preparations, the test package was assembled and ready for use.

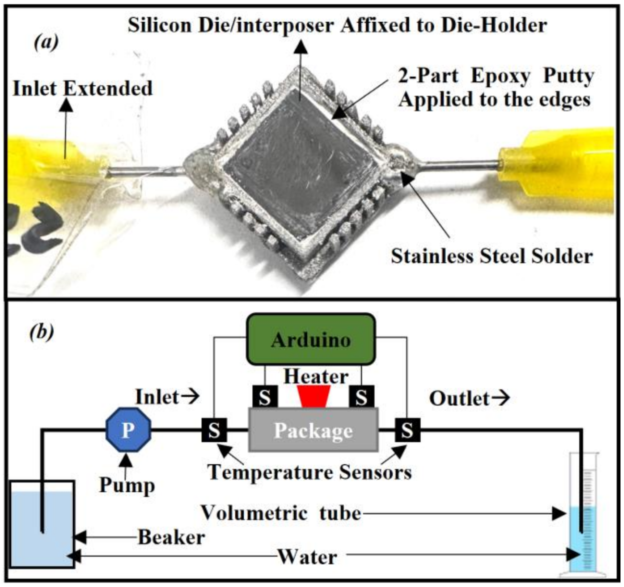

Figure 5: Package/ test sample prepared by extending the inlet/outlet and affixing silicon interposer using epoxy glue at the edges(a). Illustration demonstrating the test setup to measure the thermal resistance (ratio of increase in temperature with respect to ambient and heat flux) with heater, temperature sensors, Arduino-based data acquisition system, and flow system with peristaltic pump (b).

The test package, also referred to as the device under test (DUT), was positioned on a polylactic acid (PLA) platform fabricated using fused deposition modeling (FDM) additive manufacturing. A central cartridge heater was installed to apply a heat load to the silicon interposer surface, while four NTC thermistors were affixed to the top PLA cover to measure the average temperature of the silicon surface. Additional thermistors were added to measure the temperature of the fluid inlet and outlet flow. All the thermistors were calibrated using data provided by the manufacturer and their resistive values were then measured by an Arduino-based temperature reader. These thermally responsive parts with the microcontroller constituted the data acquisition system (DAQ).

The PLA fixture serves not only to hold the components in place but also to provide thermal isolation from the surroundings. The inlet extension was connected to the outlet of a peristaltic pump via silicone tubing, while the outlet extension allowed water to flow into a volumetric glass tube for flow rate measurement.

EXPERIMENTAL RESULTS

Data in the form of temperature and flow rate calculations were measured and recorded following the guidance of prior work [11]. Figure 6 graphically illustrates the water flow rates corresponding to different pump powers for each sample, providing a visual representation of the comparative flow resistances among them. It is evident that the Tear-Drop Pin Fin (TDPF) configuration exhibits

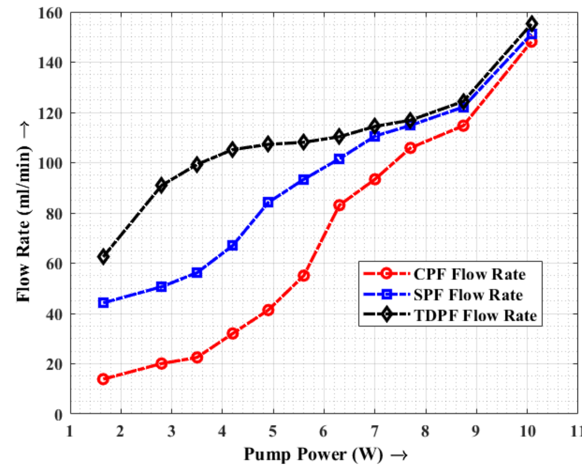

Figure 6: Flow rate in the microfluidics as a function of pump power for circular (CPF), square (SPF), and teardrop pin-fin (TDPF).

the least flow resistance among all samples, showcasing its superior fluid dynamics performance.

In Figure 7, the thermal resistance is plotted against pump power for each sample, offering insights into respective thermal performances of each package pin type. The data suggests that the TDPF pin structure surpassed the other three configurations in terms of thermal efficiency. This finding demonstrates the superior thermal management capabilities of the TDPF design compared to others.

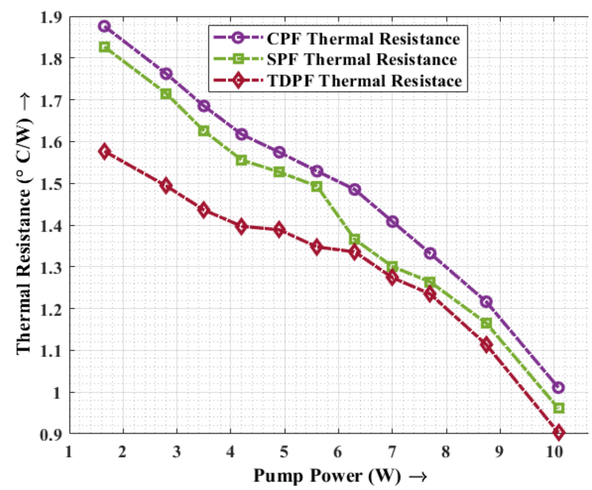

Figure 7: Thermal Resistance in the microfluidics as a function of pump power for circular (CPF), square (SPF), and teardrop pin-fin (TDPF).

An important observation emerges from these findings: the TDPF design effectively reduces thermal resistance from 5.25°C/W, as observed in a conventional non-microfluidic package, to 0.9°C/W. This significant reduction demonstrates the superior performance of the TDPF structure on thermal management efficacy, promising enhanced performance and reliability in semiconductor packaging applications. In Figure 8, the measured thermal resistances of the three pin-fin configurations in this work are compared to our previous microfluidic channel designs [10] as a function of the fluid contact area with the interposer die. It can be

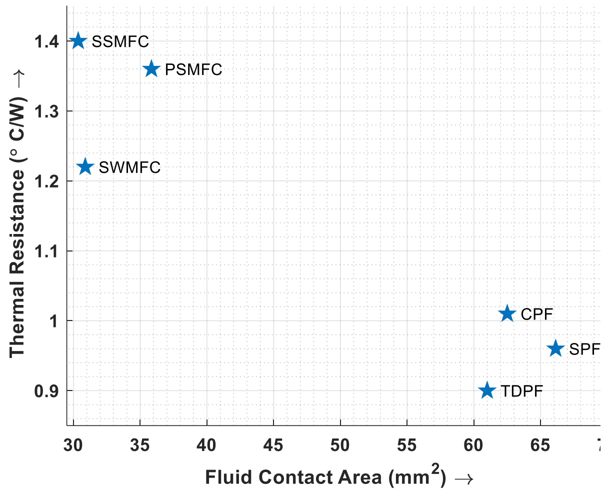

Figure 8: Comparison of the measured thermal resistance as a function of fluid contact area. The serpentine straight microfluidic channel (SSMFC), parallel straight microfluidic channel (PSMFC), serpentine wavy microfluidic channel (SWMFC) geometries are detailed in [10]. In this work, the circular (CPF), square (SPF), and teardrop pin-fin (TDPF) designs are all observed to offer thermal resistances, likely due to the increased fluid contact with the die, compared to a fluidic channel configuration.

observed that all three pin-fins outperformed fluidic channels, where this is likely driven by the increased fluidic contact for thermal transport. For applications where maximum heat removal is required, a pin-fin approach appears to yield the best performance. However, in the pin-fin design there is decreased metal package contact with the microsystems die, which may deteriorate cooling performance in a passive cooling regime, or in the event that the cooling fails, and air is present in the fluidic channels. Accordingly, the exact fluidic cooling design must be carefully considered depending on the thermal management and operational requirements of the system.

CONCLUSION

It is shown that reducing the number of thermal interfaces directly impacts the overall thermal resistance. These findings also show that DMLS is feasible for printing electronic packaging. As 2.5D and 3D chips begin to dominate the semiconductor markets these packages can be optimized to accept new shapes and even volumetric designs enabling flexibility without the cost of retooling. In this work we have demonstrated 3D printed metal microfluidic packages with a thermal resistance of 0.9°C/W for the first time, demonstrating the utility of this approach as a potential solution to address the thermal management issues facing modern microelectronic systems/ By applying microsystems technologies to electronic packaging, new paradigms of 3D electronic packaging can be realized to meet the increasing demands of electronics and microsystems alike.

ACKNOWLEDGEMENTS

This material is based upon work supported by the Department of Energy (National Nuclear Security Administration) under Award Number DE-NA0004110 and the Air Force Office of Scientific Research under award number FA9550-23-1-0477.

REFERENCES

[1] K. Olukotun, B. A. Nayfeh, L. Hammond, K. Wilson, and K. Chang, "The case for a single-chip multiprocessor," *ACM SIGPLAN Not.*, vol. 31, no. 9, pp. 2–11, Sep. 1996, doi: 10.1145/248209.237140.

[2] Y. Qin *et al.*, "Thermal management and packaging of wide and ultra-wide bandgap power devices: a review and perspective," *J. Phys. Appl. Phys.*, vol. 56, no. 9, p. 093001, Mar. 2023, doi: 10.1088/1361-6463/acb4ff.

[3] Yaman. M. Manaserh *et al.*, "Degradation of Fan Performance in Cooling Electronics: Experimental Investigation and Evaluating Numerical Techniques," *Int. J. Heat Mass Transf.*, vol. 174, p. 121291, Aug. 2021, doi: 10.1016/j.ijheatmasstransfer.2021.121291.

[4] F.-C. Chou, J. R. Lukes, and C.-L. Tien, "Heat Transfer Enhancement by Fins in the Microscale Regime," *J. Heat Transf.*, vol. 121, no. 4, pp. 972–977, Nov. 1999, doi: 10.1115/1.2826088.

[5] D. Tuckerman and R. F. W. Pease, "High-performance heat sinking for VLSI," *Electron Device Lett. IEEE*, vol. 2, pp. 126–129, Jun. 1981, doi: 10.1109/EDL.1981.25367.

[6] T. P. Jaiswal and D. S. M. Lawankar, "Fabrication of Microchannels Heat Exchanger: A review," vol. 9, no. 6, 2021.

[7] S. Scott and Z. Ali, "Fabrication Methods for Microfluidic Devices: An Overview," *Micromachines*, vol. 12, no. 3, p. 319, Mar. 2021, doi: 10.3390/mi12030319.

[8] S. Prakash and S. Kumar, "Fabrication of microchannels: A review," *Proc. Inst. Mech. Eng. Part B J. Eng. Manuf.*, vol. 229, no. 8, pp. 1273–1288, Aug. 2015, doi: 10.1177/0954405414535581.

[9] A. Joy, S. K.V., and B. Baby, "Review on fabrication and experimental study of microchannel heat sinks for cooling of electronic components," *Mater. Today Proc.*, vol. 72, pp. 2985–2991, 2023, doi: 10.1016/j.matpr.2022.08.186.

[10] B. Lohani, S. D. Hossain, and R. C. Roberts, "Dielectric Transfer Process for 3D Printed Metal Microsystems," *J. Microelectromechanical Syst.*, vol. 29, no. 5, pp. 972–977, Oct. 2020, doi: 10.1109/JMEMS.2020.3005090.

[11] B. Lohani, P. Sanchez, and R. C. Roberts, "Comparative Study of Different Microchannels for Microfluidic Packages with Integrated Thermal Management in Power Applications," in *2023 IEEE 22nd International Conference on Micro and Nanotechnology for Power Generation and Energy Conversion Applications (PowerMEMS)*, Abu Dhabi, United Arab Emirates: IEEE, Dec. 2023, pp. 214–217. doi: 10.1109/PowerMEMS59329.2023.10417154.

[12] B. Lohani, S. D. Hossain, and R. C. Roberts, "Metal Additive Microfabrication of System-in-Package with Embedded Microfluidic Thermal Management for Heterogeneous Integration with Semiconductor Dies," *J. Electron. Mater.*, Feb. 2023, doi: 10.1007/s11664-023-10256-6.

[13] B. Lohani, S. D. Hossain, and R. C. Roberts, "Metal Additively Microfabricated SiPs with Embedded Microfluidic Cooling Towards Heterogeneous Integration with SoCs," in *2023 IEEE 73rd Electronic Components and Technology Conference (ECTC)*, Orlando, FL, USA: IEEE, May 2023, pp. 1622–1626. doi: 10.1109/ECTC51909.2023.00275.

CONTACT

Ryan Price, tel: +1-915-493-1226; rmprice@miners.utep.edu